Kidney360

Acute Intravenous NaCl and Volume Expansion Reduces Sodium-Chloride Cotransporter Abundance and Phosphorylation in Urinary Extracellular Vesicles

Aihua Wu,[1] *Martin J. Wolley*,[1,2] *Qi Wu*,[3] *Diane Cowley*,[1] *Johan Palmfeldt*,[4] *Paul A. Welling*,[5] *Robert A. Fenton*,[3] *and Michael Stowasser*[1]

Key Points

- Volume expansion induced a clear reduction in aquaporin 2 abundance in urinary extracellular vesicles.
- Changes in sodium-chloride cotransporter (NCC) and phosphorylated NCC may have been primarily due to diluted post-test urine samples and stable plasma potassium during the test.

Abstract

Background Sodium chloride (NaCl) loading and volume expansion suppress the renin-angiotensin-aldosterone system to reduce renal tubular reabsorption of NaCl and water, but effects on the sodium-chloride cotransporter (NCC) and relevant renal transmembrane proteins that are responsible for this modulation in humans are less well investigated.

Methods We used urinary extracellular vesicles (uEVs) as an indirect readout to assess renal transmembrane proteins involved in NaCl and water homeostasis in 44 patients with hypertension who had repeatedly raised aldosterone/renin ratios undergoing infusion of 2 L of 0.9% saline over 4 hours.

Results When measured by mass spectrometry in 13 patients, significant decreases were observed in NCC (median fold change [FC]=0.70); pendrin (FC=0.84); AQP2 (FC=0.62); and uEV markers, including ALIX (FC=0.65) and TSG101 (FC=0.66). Immunoblotting reproduced the reduction in NCC (FC=0.54), AQP2 (FC=0.42), ALIX (FC=0.52), and TSG101 (FC=0.55) in the remaining 31 patients, and demonstrated a significant decrease in phosphorylated NCC (pNCC; FC=0.49). However, after correction for ALIX, the reductions in NCC (FC=0.90) and pNCC (FC=1.00) were no longer apparent, whereas the significant decrease in AQP2 persisted (FC=0.62).

Conclusion We conclude that (*1*) decreases in NCC and pNCC, induced by acute NaCl loading and volume expansion, may be due to diluted post-test urines; (*2*) the lack of change of NCC and pNCC when corrected for ALIX, despite a fall in plasma aldosterone, may be due to the lack of change in plasma K^+; and (*3*) the decrease in AQP2 may be due to a decrease in vasopressin in response to volume expansion.

KIDNEY360 3: 910–921, 2022. doi: https://doi.org/10.34067/KID.0000362022

Introduction

Alterations in distal tubular sodium (Na^+) handling and extracellular fluid volume have profound effects on BP, mainly due to the unique capability of the distal tubule segments to respond to hormonal stimuli and the contents of the tubular lumen (1). Accumulating data have suggested that potassium (K^+) may be a key factor in extracellular fluid volume and BP maintenance through a proposed "renal-K^+ switch" modulating the thiazide-sensitive Na^+-chloride (Cl^-) cotransporter (NCC) (2). Reduced plasma K^+ concentration ($[K^+]$) is associated with increased abundance and activity of NCC in the distal convoluted tubule (3), whereas oral KCl supplementation has the capacity to limit the increase in NCC abundance induced by mineralocorticoids in both humans and mice (4,5). These alterations are also accompanied by downregulation of the Na^+-independent Cl^-/bicarbonate (HCO_3^-) exchanger pendrin (6).

In contrast to the negative regulatory role of K^+ on NCC, we and others have suggested that aldosterone plays a stimulatory role (5,7,8). In patients with

[1]Endocrine Hypertension Research Centre, University of Queensland Diamantina Institute, Greenslopes and Princess Alexandra Hospitals, Brisbane, Australia
[2]Department of Nephrology, Royal Brisbane and Women's Hospital, Brisbane, Australia
[3]Department of Biomedicine, Aarhus University, Aarhus, Denmark
[4]Department of Clinical Medicine, Aarhus University, Aarhus, Denmark
[5]Department of Medicine and Physiology, Johns Hopkins University, Baltimore, Maryland

Correspondence: Prof. Michael Stowasser, Endocrine Hypertension Research Centre, The University of Queensland Diamantina Institute, Greenslopes and Princess Alexandra Hospitals, 199 Ipswich Road, Woolloongabba, QLD 4102, Brisbane, Australia. Email: m.stowasser@uq.edu.au

primary aldosteronism (PA), undergoing 4-day administration of exogenous mineralocorticoid was associated with increases in NCC and phosphorylated NCC (pNCC), whereas plasma K^+ inversely correlated with NCC and pNCC at baseline (5). In another group of patients, although increases in NCC and pNCC were not observed, the inverse correlations with plasma K^+ were replicated (6). However, interpretation of the findings of the two studies was complicated by the fact that they involved (*1*) exogenous mineralocorticoid administration, (*2*) KCl supplementation, and (*3*) oral NaCl loading.

PA is a common, specifically treatable, and potentially curable form of hypertension, characterized by excessive and autonomous production of aldosterone by the adrenal glands. Seated saline suppression testing (SSST) is a highly sensitive, reliable, yet relatively simple, method of confirmatory testing that has a low rate of inconclusive results when compared with the more time-consuming and laborious fludrocortisone suppression test (9,10). During SSST, subjects with hypertension who have elevated aldosterone/renin ratios (ARRs) undergo intravenous infusion of 2 L of 0.9% saline over 4 hours while patients are maintained in the seated position. In subjects without PA, the acute NaCl loading and volume expansion during SSST, by suppressing renin (and, consequently, the chronic aldosterone regulator angiotensin II), leads to suppression of plasma aldosterone, whereas plasma aldosterone remains unsuppressed in patients with PA.Urinary extracellular vesicles (uEVs) are a tool to assess renal epithelial cell function in humans (7,11). A recent, large-scale, unbiased analysis identified uEV proteins that track the abundance of the parent protein in the kidney (12), further supporting the reliability of using uEV protein changes to monitor specific physiologic responses and disease mechanisms.

In this observational study, we took advantage of the more simplified nature of the SSST, which involved only NaCl loading and used the noninvasive approach of examining uEVs (13–15), to (*1*) explore the effects of NaCl loading and volume expansion on renal transmembrane proteins involved in salt and volume homeostasis, using quantitative mass spectrometry (liquid chromatography with tandem mass spectrometry [LC-MS/MS]); (*2*) validate LC-MS/MS findings in a larger sample size by immunoblotting; and (*3*) define the role (if any) of NaCl loading alone on NCC abundance and phosphorylation in patients with hypertension and raised ARRs.

Materials and Methods

Detailed methods are demonstrated in the Supplemental Appendix 1. Briefly, from April 2017 to August 2020, a total of 44 (29 female [F29]/15 male [M15]) patients with hypertension and raised ARRs were invited and all agreed to participate. All participants underwent SSST to confirm or exclude the diagnosis of PA. At least 4 weeks before SSST, medications affecting plasma aldosterone and renin levels were withdrawn and replaced by other antihypertensive medications, including verapamil, prazosin, or doxazosin, moxonidine, and/or hydralazine. Patients undergoing SSST were admitted to hospital to ensure the dietary (normal hospital diet) and posture requirement were met and to facilitate monitoring of plasma K^+ and other parameters. SSST involved intravenous infusion of 2 L of 9% saline over 4 hours in a seated position, and assessment of plasma aldosterone concentration, direct renin concentration, and cortisol concentration at baseline and at the end of the infusion (10,16,17). Midstream urines were collected before SSST at 7 AM (basal) and 1-hour postcompletion (post) of the saline infusion. uEVs were isolated using progressive ultracentrifugation, as previously described (5). uEVs were characterized and analyzed by quantitative tandem mass tag (TMT)–labeled LC-MS/MS (6,18) or immunoblotting. A list of abbreviations was included to assist reader (Supplemental Table 3).

Ethical Issues

The SSST was performed in the Hypertension Units of the Princess Alexandra Hospital (Brisbane, Australia). The laboratory investigations were performed in the Endocrine Hypertension Research Centre, The University of Queensland Diamantina Institute (Brisbane, Australia) and the Department of Biomedicine, Aarhus University (Aarhus, Denmark). Ethical approval was granted by the Metro South Human Research Ethics Committee (clinical trials repository identifier: CT-2018-CNT-03504-1 v1).

Bioinformatic and Statistical Analyses

Calculations were processed with R. Overlap analyses were performed using Vesiclepedia and ExoCarta protein databases to compare the mass spectrometry dataset with other human urine studies and to identify EV-enriched proteins. A rat renal transporter protein database was used to identify renal transmembrane proteins (19). Gene Ontology (GO) analysis was performed using the ClueGO plugin (version 2.5.5) in the Cytoscape environment (version 3.7.2), and gene lists corresponding to 878 differentially expressed proteins (DEPs) were used as input. GO terms were updated on June 11, 2020.

In TMT-labeled LC-MS/MS, protein ratios obtained with the aid of the universal control channel TMT 126 were $\log_2$ transformed. In immunoblotting, protein absolute abundances were analyzed by Image J software. To minimize operation errors occurring during gel loading and transferring, relative protein abundance was applied to allow comparison between blots, which was determined as dividing the protein absolute abundance by a ratio that was obtained from normalization of EV marker protein apoptosis-linked gene 2-interacting protein X (ALIX) in the control sample loaded on each blot. The relative protein abundance was then $\log_{10}$ transformed.

For paired comparisons before and after SSST, Wilcoxon tests were performed to compare the differences of biochemical parameters, and *t* tests were performed to compare the differences of protein ratios/relative abundance. In TMT-labeled LC-MS/MS, a DEP was identified as that with $P<0.05$, false discovery rate of <0.1, and fold change (FC) of ≥ 1.20 or ≤ 0.83. Pearson correlations were assessed to seek correlations between protein ratios/abundances and biochemical parameters. A P value <0.05 was considered statistically significant. Protein data are presented as median (range), unless stated otherwise.

Results

Participants' Clinical Features during SSST

A total of 44 participants (F29/M15) were recruited (screening features and use of antihypertensive drugs are listed in Supplemental Table 1) and completed SSST. The number of participants at each stage of analyses is summarized in Supplemental Figure 1. SSST was positive in 34 participants (F19/M15), thereby confirming PA. SSST was negative in 10 participants (F10/M0), for which PA was excluded, and these participants were designated to have low renin essential hypertension (LRH). Participants' clinical characteristics and biochemical changes during SSST is summarized in Table 1. Significant decreases in plasma concentrations of aldosterone and renin were observed in both subjects with PA and those with LRH, demonstrating the suppressive effect of SSST on the renin-angiotensin-aldosterone system. Plasma ARR decreased, but its decrease in PA was NS, reflecting the autonomous aldosterone overproduction in PA. A reduction in plasma cortisol in both participants with PA and those with LRH occurred between 7 AM and the completion time of SSST (12 PM), in keeping with the known fall in adrenocorticotrophic hormone as part of its normal circadian rhythm during this time period. There were no changes in plasma [K^+] in patients with either PA or those with LRH, but a significant increase in plasma [Cl^-] (probably due to infusion of NaCl) and a nonsignificant trend toward a decrease in plasma [HCO_3^-] in both subjects with PA and those with LRH. Plasma copeptin fell during SSST (significantly among the total cohort and the PA subgroup), reflecting a decrease in circulating arginine vasopressin induced by volume expansion during SSST. Spot urine creatinine fell significantly in both subjects with PA and those with LRH. BPs during SSST were measured in all but one (patient 39). Systolic and diastolic BPs did not change significantly in the 34 participants (F19/M15) with PA, the 10 participants (F10/M0) with LRH, or in the combined cohort of 44 individuals.

Characterization of uEVs

Due to the limited amount of uEVs obtained from participants, nine uEVs isolated from two healthy volunteers at different times on multiple days were characterized by both nanoparticle tracking analysis and the presence of marker proteins using immunoblotting. The diameter of the uEV particles from the nine uEVs ranged overall from 25.5 to 999.5 nm, with the mean±SD particle size for each of the nine samples ranging from 218.9±1.6 to 341.7±5.9, and mode particle size from 139.9±7.0 to 194.9±6.7 nm (Figure 1, A–C, Supplemental Table 2). Immunoblotting detected the most frequently used uEV marker, ALIX, in all nine uEV samples, and tumor susceptibility gene 101 (TSG101) and tetraspanin CD9 (CD9) in most samples (Figure 1D).

Patients' uEV samples were characterized by the presence of EV-enriched proteins. LC-MS/MS quantified 99 proteins isolated from 13 (ten with PA [PA10]/three with LRH [LRH3], F8/M5) patients' uEVs that were among the list of the top 100 EV-enriched proteins published on Vesiclepedia, including the widely used EV markers (Figure 1E, Supplemental Appendix 2). Immunoblotting detected ALIX in uEVs isolated from 31 (F21/M10, PA24/LRH7) subjects, and detected TSG101 from 27 (F17/M10, PA22/LRH5) subjects (Supplemental Figure 5). We observed a shift in the ALIX bands in multiple samples in immunoblots, but no size shifts for other proteins in the same samples. Despite ALIX truncation by the ESCRT machinery (20), our main hypothesis is that this may be related to Tamm–Horsfall protein, which was also observed in a recent study (21).

Proteomic Analyses

Among the 13 participants subjected to TMT-labeled LC-MS/MS, a total of 3307 proteins were identified, of which 3007 proteins were quantifiable (Supplemental Appendix 2; a simplified version can be directly accessed at http://interpretdb.au.dk/database/SSST/SSST_proteome.html). Comparison of proteins quantified in this study and other human uEV and urinary exosome databases demonstrated 79% overlap with the uEV database Vesiclepedia, 73% overlap with the urinary exosome database ExoCarta (Figure 2A), and 104 renal transporter proteins were identified in the uEVs (Figure 2A).

A total of 878 DEPs were identified (Figure 2B, Supplemental Appendix 2), with 636 increased and 242 decreased in abundance after SSST. Of these, 294 DEPs were quantified in all paired uEV samples, but there were no apparent differences between subjects with PA and those with LRH, as demonstrated using an unsupervised hierarchic clustering heat map (Supplemental Figure 2). Of the 294 DEPs, 29 were identified as EV-enriched proteins (Figure 1E), and 12 were renal transmembrane proteins (Table 2). Decreases in NCC, pendrin, and aquaporin 2 (AQP2) were notable due to their involvement in NaCl and water homeostasis. However, significant decreases in the widely used uEV markers (*e.g.*, ALIX, FC=0.65 [0.43–1.60]; TSG101, FC=0.66 [0.39–1.40]; CD63, FC=0.77 [0.34–1.29]) were also observed, implying changes in exosomal biogenesis and secretion. Although epithelial Na^+ channel subunits were not detected in this experiment, prostasin was identified in all uEV samples, which was an assumed indicator of full epithelial Na^+ channel activity/cleavage (22,23), but its level did not change during SSST.

GO enrichment suggested upregulated DEPs were closely associated with cell components, including the mitochondrial matrix (22%), whereas the downregulated DEPs were associated with cytoplasmic vesicles (38%). In the biologic process category, the upregulated DEPs were associated with establishment of location in cell (25%), whereas downregulated DEPs were associated with secretion by cell (32%) (Supplemental Figure 3).

Among the three transmembrane DEPs of interest, plasma [K^+] negatively correlated with pendrin (R^2=0.23, P=0.01) and plasma copeptin positively correlated with AQP2 (R^2=0.7, P=0.01), but these correlations were on the basis of only eight plasma copeptin measurements in five participants. We did not observe clear correlations between NCC and plasma aldosterone or K^+, unlike in our previous study using immunoblotting (Supplemental Figure 4) (5).

Immunoblotting Validation of Decreases in NCC and AQP2

Due to the limited amount of uEVs, immunoblotting measured abundances of NCC, pNCC, and ALIX in uEVs

Table 1. Participants' characteristics and changes in biochemical factors during seated saline suppression testing

Characteristic	Normal Range in Adults	Screening Value	PA (n=34, Female 19/Male 15)			Low Renin Hypertension (n=10, F10/M0)		
			Basal	Post	P Value[a]	Basal	Post	P Value[a]
Screening measurements (n=44)								
Age, yr		51.9±11.0						
Female/male, n/n		29/15						
Weight, kg		89.3±21.2						
Height, cm		167.0±9.6						
BMI, kg/m^2	18.5–24.9	31.9±6.4						
Number of anti-HTN drugs		1.7±1.1						
SBP/DBP, mm Hg	<140/90	146.3±18.0/86.6±14.9						
eGFR, ml/min	>60	96.7±12.7						
Plasma creatinine, μmol/L	45–90	67.2±15.8						
Diagnosis								
PA/LRH, n/n		34/10						
Measurements during SSST								
Plasma aldosterone, pmol/L	100–950		615.9±515.0	426.9±421.2	9.1×10^{-4}	479.0±327.0	129.9±85.5	0.002
Plasma renin, mU/L	8–40		3.5±2.1	2.8±1.8	0.002	7.3±7.4	4.2±3.8	0.01
Plasma ARR, pmol/mU	2–75		231.0±305.3	188.2±150.6	0.40	128.1±128.4	51.9±48.3	<0.01
Plasma cortisol, nmol/L	8 AM 140–6404 PM 80–440		325.1±99.1	164.0±57.5	2.8×10^{-6}	358.8±179.9	149.4±65.7	0.002
Plasma K^+, mmol/L	3.5–5.2		3.67±0.42	3.74±0.37	0.20	3.93±0.36	3.90±0.22	0.73
Plasma Cl^-, mmol/L[b]	95–110		96.3±2.8	100.0±3.2	2.1×10^{-6}	96.0±2.5	100.6±3.5	0.004
Plasma HCO_3^-, mmol/L[b]	22–2		23.3±6.0	22.4±6.0	0.10	22.7±4.9	21.3±5.3	0.08
Plasma copeptin, pmol/L[c]			8.8±6.8	6.6±6.5	0.02	5.2±4.6	3.1±1.8	0.25
SBP, mm Hg	<140		142.0±24.6	146.6±20.7	0.17	139.3±20.4	141.0±15.1	0.65
DBP, mm Hg	<90		83.9±12.9	85.8±13.3	0.29	82.1±13.8	78.8±11.7	0.55
Spot urine creatinine, mg/dl[c]			108.7±45.6	35.3±22.9	9.3×10^{-10}	94.8±65.2	36.2±21.1	0.02

Values are the mean±SD unless otherwise noted. SSST, seated saline suppression testing; PA, primary aldosteronism; basal, baseline measurement before SSST commencement; post, measurement at SSST completion; BMI, body mass index; SBP, systolic BP; DBP, diastolic BP; ARR, aldosterone/renin ratio; Cl^-, chloride; HCO_3^-, bicarbonate; F, female; M, male; LRH, low renin hypertension.

[a]P values by paired Wilcoxon test (post/basal).

[b]Paired plasma Cl^- and HCO_3^- was measured in 41 participants (PA31, F18/M13; LRH10, F10/M0).

[c]Paired plasma copeptin was measured in 33 participants (PA25, F14/M11; LRH8, F8/M0).

[d]Paired spot urine creatinine was measured in 39 participants (PA32, F18/M14; LRH7, F7/M0).

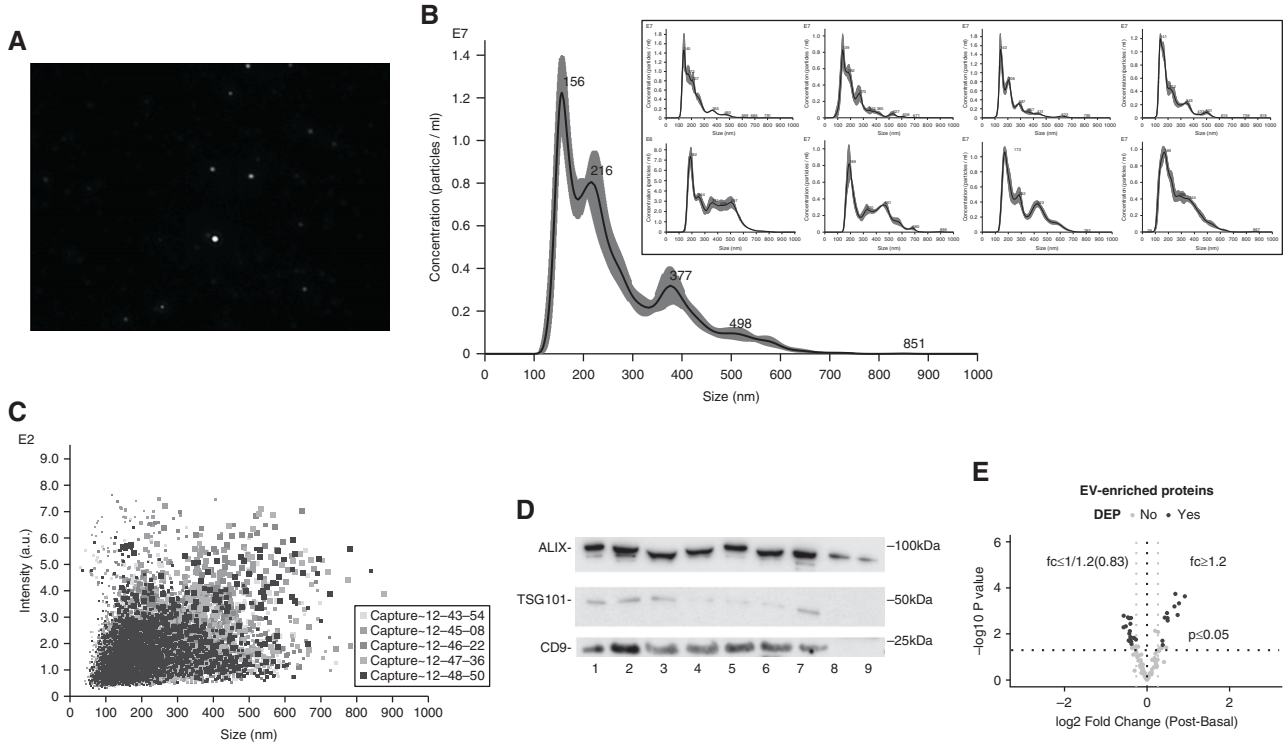

Figure 1. | **Successful characterization of urinary extracellular vesicles (uEVs).** (A) Screenshot from a diluted uEV sample (1:1000) revealing a range of particle sizes. (B) Concentrations (particle per milliliter) of the uEV sample in (A) (expressed as averaged finite track length adjustment concentration, the remaining eight uEV samples displayed in box). (C) Nanoparticle-tracking analysis depicting the nanoparticle size density of the uEV sample in (A). (D) Immunoblotting of uEV-enriched proteins (apoptosis-linked gene 2-interacting protein X [ALIX], tumor susceptibility gene 101 [TSG101], and tetraspanin CD9 [CD9]) in nine different uEV samples isolated from two healthy volunteers collected at different time on multiple days. (E) Volcano plot of uEV-enriched proteins detected by quantitative tandem mass tag labelled liquid chromatography tandem mass spectrometry. Basal, before seated saline suppression testing at 7 AM; DEP, differentially expressed protein; post, 1-hour postcompletion of saline infusion; fc, fold change.

isolated from 31 subjects (F21/M10, PA24/LRH7), and abundances of AQP2 and TSG101 in uEVs from 19 (F12/M7, PA17/LRH2) and 27 (F17/M10, PA22/LRH5) subjects, respectively (Figure 3, Supplemental Figure 5). Immunoblotting reproduced the significant decreases in the relative abundances of NCC (FC=0.54 [0.02–3.72], $P<0.001$) and AQP2 (FC=0.42 [0.009–2.00], $P=0.003$) observed with LC-MS/MS. A reduction was also observed in the abundance of pNCC (FC=0.49 [0.02–2.15], $P<0.001$), whereas no apparent change was detected in the pNCC/NCC ratio (FC=1.10 [0.11–4.20], $P=0.31$) (Figure 4). The accompanying decreases in the uEV marker ALIX (FC=0.52 [0.05–7.29], $P<0.001$) and TSG101 (FC=0.55 [0.13–3.63], $P<0.001$) were also reproduced (Figure 4), which again raised the possibility that decreases in the abundances of proteins of interest may be due to decreased uEV concentration.

After correction for spot urine creatinine concentrations, decreases were replaced with small increases for NCC (FC=1.72 [0.03–56.27], $P=0.06$), pNCC (FC=1.59 [0.04–20.18], $P=0.06$), ALIX (FC=2.00 [0.08–11.86], $P=0.007$), and TSG101 (FC=1.62 [0.21–8.96], $P=0.01$), and AQP2 (FC=0.99 [0.07–5.18], $P=0.94$) did not change (Figure 4). After correcting relative protein abundances for the uEV marker ALIX, the decreases in NCC (FC=0.90 [0.13–7.19], $P=0.31$) and pNCC (FC=1.00 [0.16–5.04], $P=0.52$) were abolished, whereas the decrease in AQP2 remained significant (FC=0.62 [0.03–3.79], $P=0.04$) (Figure 4).

Plasma [K^+] Inversely Correlated with NCC and AQP2

Plasma [K^+] inversely correlated with NCC abundance ($R^2=0.07$, $P=0.02$; Figure 5), and this correlation remained after correction for the uEV marker ALIX ($R^2=0.08$, $P=0.02$), but not after correction for spot urine creatinine concentration ($R^2=0.06$, $P=0.07$). Besides, plasma [K^+] inversely correlated with AQP2 ($R^2=0.22$, $P=0.002$), and this correlation remained significant after correction for ALIX ($R^2=0.26$, $P<0.001$) and correction for urine creatinine ($R^2=0.21$, $P=0.008$) (Figure 5). No clear correlation was detected between plasma [K^+] and pNCC abundance, unlike in our previous observations (Supplemental Figure 6) (5).

Plasma aldosterone appeared to positively correlate with AQP2 ($R^2=0.11$, $P=0.04$) and the ALIX-corrected abundance of AQP2 ($R^2=0.10$, $P=0.04$). Plasma copeptin positively correlated with AQP2 ($R^2=0.34$, $P=0.0002$) and the ALIX and urine creatinine–corrected AQP2 ($R^2=0.36$, $P=0.0001$ and $R^2=0.21$, $P<0.008$, respectively) (Figure 5). Plasma [Cl^-] showed trends toward positive correlations with creatinine-corrected pNCC ($R^2=0.06$, $P=0.08$), and ALIX-corrected NCC ($R^2=0.05$, $P=0.09$) and pNCC ($R^2=0.06$, $P=0.06$) (Supplemental Figure 6).

Discussion

The primary aim of this study was to use large-scale proteomic techniques to investigate the effect of acute NaCl

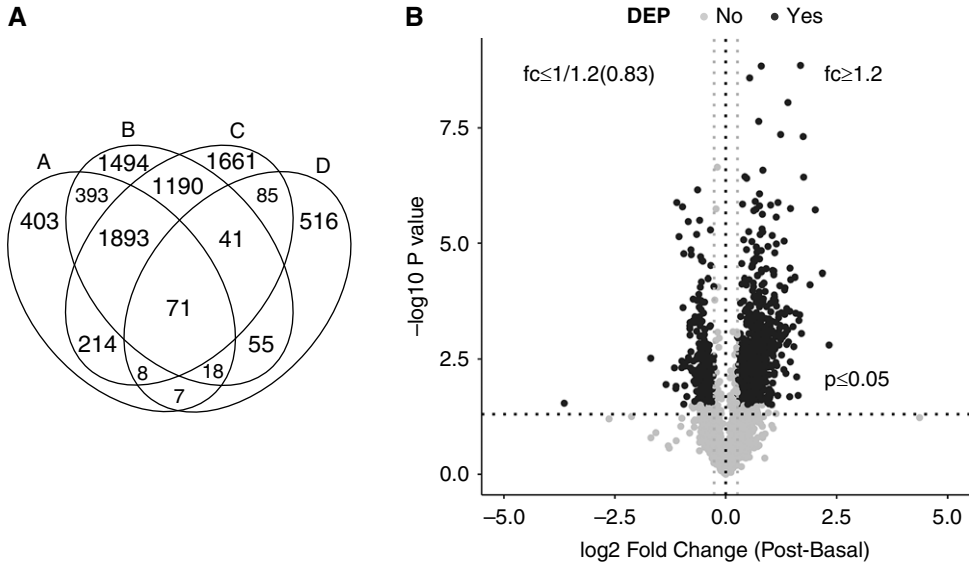

Figure 2. | **Overview of overlapping analysis and differential expression analysis.** (A) Venn diagram summarizing quantified proteins (represented as A) and their overlaps with Vesiclepedia (represented as B), ExoCarta (represented as C), and a renal transport protein database (represented as D). (B) Volcano plot depicting differentially abundant proteins affected by seated saline suppression testing (SSST) in 13 participants. Proteins quantified in four or more samples were used as input. The $-\log_{10} P$ value (paired t test with 95% CI) is plotted against the mean $\log_2$ fold change (mean of [$\log_2$ post ratio$-\log_2$ basal ratio]). The nonaxial horizontal dotted line denotes $P=0.05$, which is the significant threshold (before logarithmic transformation). The two gray nonaxial vertical dotted lines denote fold change (fc) of 1.20 or 0.83 during SSST. The black dots represent proteins with $P<0.05$, false discovery rate of <0.1, and fc of ≥ 1.20 or ≤ 0.83 during SSST to be the DEPs, and the gray dots represent proteins not defined as DEPs. 95% confidence interval, 95% CI.

loading and volume expansion on renal transmembrane proteins in uEVs from patients with hypertension and raised ARRs. Although we did not have a sufficient quantity of all uEV samples to perform transmission electron microscopy (24), the size-distribution assessment by nanoparticle tracking analysis, coupled to the identification of widely used uEV markers, including ALIX and TSG101, suggested successful uEV isolation using progressive ultracentrifugation. This was also supported by the nonbiased LC-MS/MS data where, of the >3000 proteins identified, 99 were identified as EV-enriched proteins and >70% of them had previously been found to be present in uEVs and exosomes.

Of the proteins determined by quantitative LC-MS/MS to be altered in abundance during SSST, reductions in NCC, pendrin, and AQP2 were of interest. However, several uEV markers were also differentially expressed during SSST, suggesting the reductions in these proteins may be due to alterations in actual uEV biogenesis or excretion rates (21). To address this possibility, we validated the effects of SSST on AQP2, NCC (and its phosphorylated form), and the uEV markers ALIX and TSG101 using immunoblotting. We did not validate pendrin due to a lack of antibodies crossreacting with human pendrin. In line with the LC-MS/MS data, in both subjects with PA and those with LRH, there were decreases in NCC, AQP2, ALIX, and TSG101, and pNCC additionally showed a reduction at completion of the SSST, although the findings in subjects with LRH need validation due to small numbers.

In the Hypertension Units of Princess Alexandra Hospital, during SSST, antihypertensive drugs that have the potential to significantly affect the measurement of plasma ARR were withdrawn at least 4 weeks before SSST for diuretics (including spironolactone) and at least 2 weeks before SSST for β-blockers, clonidine, methyldopa, nonsteroidal anti-inflammatory drugs, angiotensin-converting enzyme inhibitors, angiotensin receptor blockers, and dihydropyridine calcium blockers (25). Other antihypertensive medications that have lesser effects on the ARR, including verapamil, prazosin, or doxazosin, moxonidine, and/or hydralazine, were commenced, where necessary, to ensure ongoing control of hypertension. Therefore, the likelihood that antihypertensive medications may have had significant effects on the Na^+ channels is small.

There was a large reduction observed in urine creatinine concentration. Therefore, we corrected relative protein abundances for urine creatinine concentrations and found that the apparent decreases in NCC, pNCC, ALIX, and TSG101 were replaced with mild increases and the change in AQP was no longer evident. However, correction for creatinine concentration in spot urines does not address the influence of variable uEV recovery/sedimentation rates during progressive ultracentrifugation (26). We then performed correction for the uEV marker protein ALIX. This resulted in abolition of the decreases in NCC and pNCC, whereas the decrease in AQP2 remained, and the changes in the three channels were reproduced when predicting their total contents in the collected urine by multiplying each relative abundance to total urine volume (Supplemental Figure 7). These observations raise the possibility that decreases in NCC and pNCC in uEVs observed in LC-MS/MS and immunoblots are due to reductions in uEVs, either because the concentration of uEVs is reduced after SSST (supported by the reduced urine creatinine

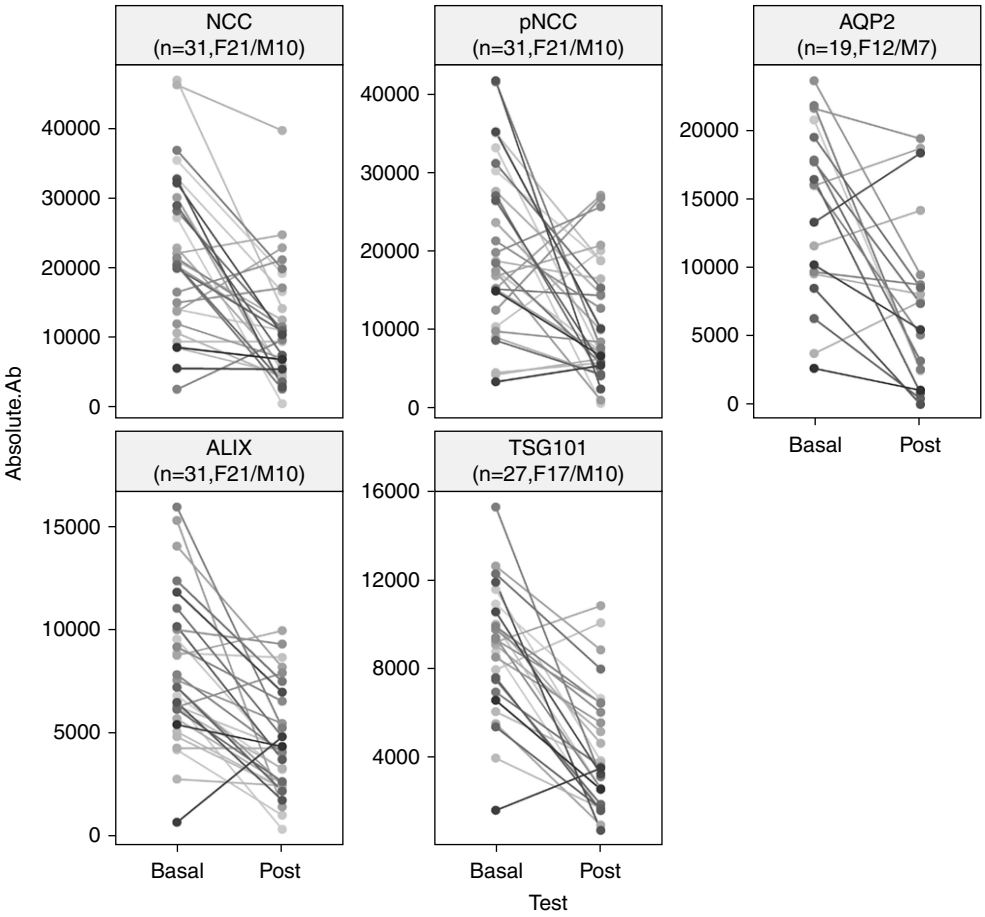

Figure 3. | **Decreases in protein absolute abundances detected by western blotting.** Line plots summarizing proteins detected by Western blot in absolute abundances (Absolute.Ab) of sodium-chloride cotransporter (NCC), phosphorylated NCC (pNCC), aquaporin 2 (AQP2), ALIX, and TSG101 in uEVs from all subjects, as a summarized presentation of Supplemental Figure 5. F, female; M, male.

concentration), or less uEVs are excreted during SSST (supported by reduced abundance of EV markers). A recent study demonstrated that water loading reduced the abundance per unit volume of EV markers but increased the amount of Tamm–Horsfall protein recovered in uEVs (21). Acute saline loading–induced increased urine volume may also result in greater excretion of albumin in the post sample compared with the baseline condition. Given that the total protein from each sample loaded on mass spectrometry (6.4 μg) or western blotting (20 μg) was the same, it is, therefore, not surprising that the readout of uEV proteins was lower after SSST. Findings of a recent study comparing uEV quantification methods suggested that urine creatinine can replace the need for uEV quantification to normalize spot urines (21). In this study, the abundance of widely used EV markers, whether quantified by mass spectrometry or immunoblotting, positively correlated with spot urine creatinine concentration (Supplemental Figure 8).

The apparent lack of changes in ALIX-corrected NCC and pNCC, despite the fall in endogenous aldosterone, may be due to the lack of change in plasma $[K^+]$ during SSST. Although aldosterone and its analogues were originally thought to be major regulators of NCC (8,27–30), plasma $[K^+]$ is suggested a more potent regulator of NCC abundance and phosphorylation (5,31–34). Sufficient dietary K^+ supplementation to maintain normokalemia in mice during aldosterone infusion reduced plasma membrane NCC (4). In this study, the weak inverse correlation of plasma $[K^+]$ with NCC is consistent with animal studies. The low R^2 value of the correlation of plasma $[K^+]$ with ALIX-corrected NCC and the unclear association between plasma $[K^+]$ and ALIX-corrected pNCC in this study may reflect the fact that, unlike in our previous studies, almost all patients' plasma $[K^+]$ fell within the normal range (3.5–5.2 mmol/L), with considerably less variation among samples, resulting in a lower power to detect their relationship.

A fall in ALIX-corrected AQP2 may reflect a fall in plasma vasopressin induced by water loading (35), as evidenced by the significant decrease in plasma copeptin in both subjects with PA and those with LRH. Reduction in AQP2 abundance may also have been due to reduced aldosterone, which is a potent stimulator of AQP2 expression independently of angiotensin II (36). Surprisingly, there was a negative correlation between plasma $[K^+]$ and creatinine-corrected AQP2 (determined by immunoblotting). Plasma $[K^+]$ usually positively correlates with kidney levels of AQP2, with K^+ deficiency rapidly resulting in nephrogenic

Table 2. Differentially expressed renal membrane proteins quantified in all samples during seated saline suppression testing (*n*=13, Female 8/Male 5, primary aldosteronism 10/low renin hypertension 3)

Number	Accession	Protein Description	Alternative Name	Gene Symbol	Fold Change (Post/Basal), Median (Range)	Trend	*P* Value[a]	False Discovery Rate
1	P55017-2	Isoform 2 of solute carrier family 12 member 3	NCC	*SLC12A3*	0.70 (0.50–1.82)	Decrease	0.03	0.091
2	P21796	Voltage-dependent anion-selective channel protein 1	VDAC-1	*VDAC1*	1.49 (0.58–4.24)	Increase	0.03	0.098
3	O95833	Chloride intracellular channel protein 3	CLIC3	*CLIC3*	1.27 (0.85–2.08)	Increase	0.003	0.023
4	P45880-1	Isoform 1 of voltage-dependent anion-selective channel protein 2	VDAC-2	*VDAC2*	1.47 (0.82–3.22)	Increase	0.003	0.022
5	Q9Y277	Voltage-dependent anion-selective channel protein 3	VDAC-3	*VDAC3*	1.58 (0.65–4.24)	Increase	0.003	0.022
6	O43511	Pendrin	Pendrin	*SLC26A4*	0.84 (0.55–1.18)	Decrease	0.007	0.040
7	P05141	ADP/ATP translocase 2	ANT2	*SLC25A5*	1.88 (0.74–4.39)	Increase	0.005	0.033
8	Q9C0H2–4	Isoform 4 of protein tweety homolog 3	TTYH3	*TTYH3*	0.61 (0.35–1.14)	Decrease	0.000	0.008
9	P41181	Aquaporin 2	AQP2	*AQP2*	0.62 (0.24–1.39)	Decrease	0.004	0.026
10	Q9NQA5	Transient receptor potential cation channel subfamily V member 5	ECaC1	*TRPV5*	0.77 (0.40–1.11)	Decrease	0.002	0.017
11	Q9NRA2	H^+/sialic acid cotransporter sialin	Sialin	*SLC17A5*	0.63 (0.25–1.61)	Decrease	0.010	0.049
12	Q00325	Phosphate carrier protein, mitochondrial	PTP	*SLC25A3*	1.66 (0.79–4.56)	Increase	0.003	0.025

basal, baseline measurement before SSST commencement; post, measurement at SSST completion; NCC, sodium-chloride cotransporter.
[a]*P* values by paired *t* test (post/basal).

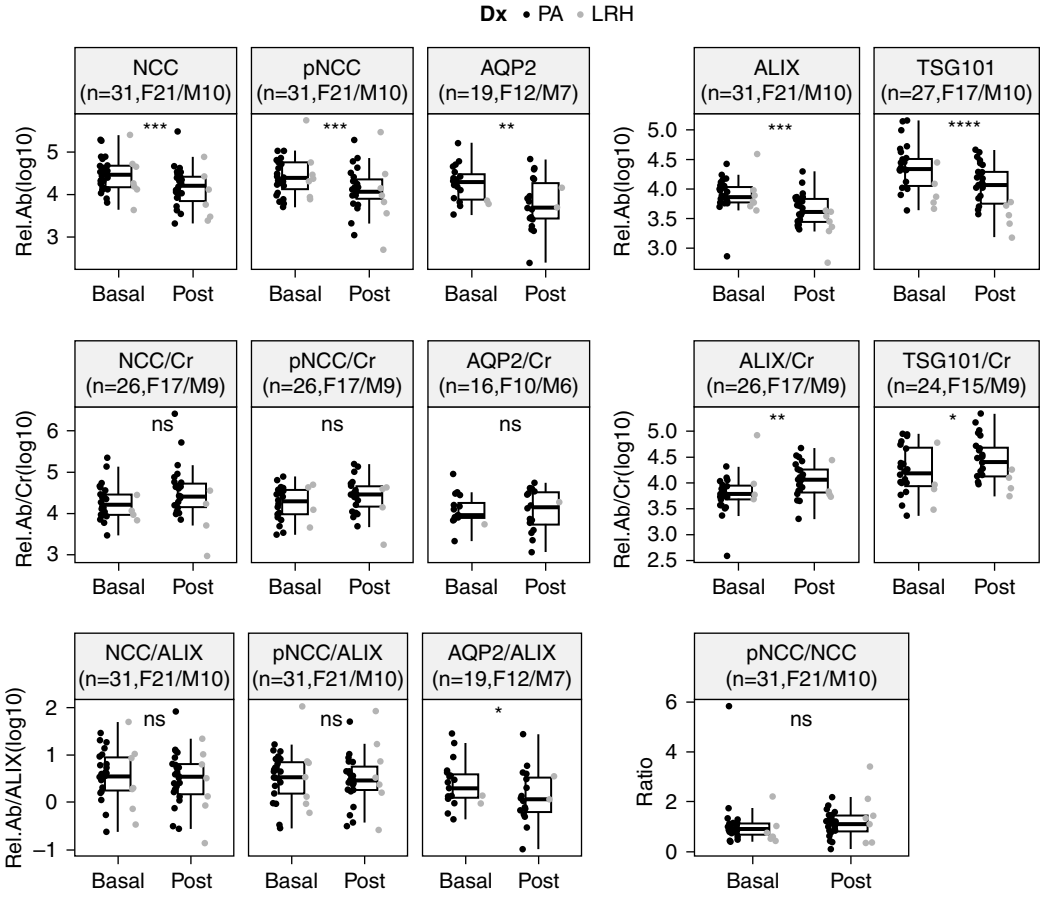

Figure 4. | **Differences in relative abundance of analyzed proteins without and with correction for urine creatinine or ALIX, and change in pNCC/NCC ratio during SSST.** Cr, urine creatinine concentration; Dx, SSST diagnosis; LRH, low renin essential hypertension; PA, primary aldosteronism; Rel.Ab, protein relative abundance; Rel.Ab/ALIX, protein relative abundance corrected for ALIX; Rel.Ab/Cr, protein relative abundance corrected for spot urine creatinine concentration. F, female; M, male.

diabetes insipidus due to autophagic degradation of AQP2 (37–39). It is possible that the increased uEV levels of AQP2 when plasma [K^+] is lower represents a cellular mechanism to remove AQP2 from principal cells during hypokalemia and may be linked to the process of autophagy (40,41).

When measured by LC-MS/MS, the negative correlation between plasma [K^+] and pendrin is consistent with our previous report (5,6). There are additional associations of the remaining nine renal transmembrane DEPs with biochemical factors (Supplemental Figure 4). The increases in voltage-dependent anion-selective channels and their positive correlations with plasma [Cl^-] may reflect the transport of Cl^- across the mitochondrial membranes and plasma membrane due to infusion of NaCl. Besides, the correlations, detected by LC-MS/MS and immunoblotting, between plasma [HCO_3^-] and several of the proteins examined require validation. The fact that [HCO_3^-] was much lower than the normal range in some patients, despite the patients being clinically well, raises the possibility of a technical issue, because processing of plasma samples for [HCO_3^-] measurement was delayed and some samples were subjected to freeze-defrost cycles before measurement.

Admittedly, the diverse origins and dynamic molecular composition of uEVs present an enormous analytic challenge. Therefore, it remains uncertain as to what extent the uEV isolation and measurement approaches used in this study and the data that they yield are able to truly reflect disturbances to physiologic processes that may occur across a range of disease scenarios. Although uEV analysis has been demonstrated to be a reliable tool to monitor specific physiologic responses (12), methods of uEV quantification and normalization need further optimization and standardization to foster scientific advances in uEV research and successful translation into clinical practice.

In summary, this is the first study to quantify changes in the protein profile of uEVs in response to acute NaCl loading and volume expansion–induced renin-angiotensin-aldosterone system inhibition in subjects with hypertension and repeatedly elevated ARRs. Volume expansion induced a clear reduction in AQP2 abundance, but changes in NCC and pNCC may have been primarily due to diluted post-SSST urine samples and a stable plasma [K^+] during the test, despite a fall in aldosterone levels. A study in a hypertensive cohort with raised ARRs whose plasma [K^+] decreased post-SSST (42) is required to further elucidate if plasma [K^+] contributes to the variations in NCC abundance and phosphorylation.

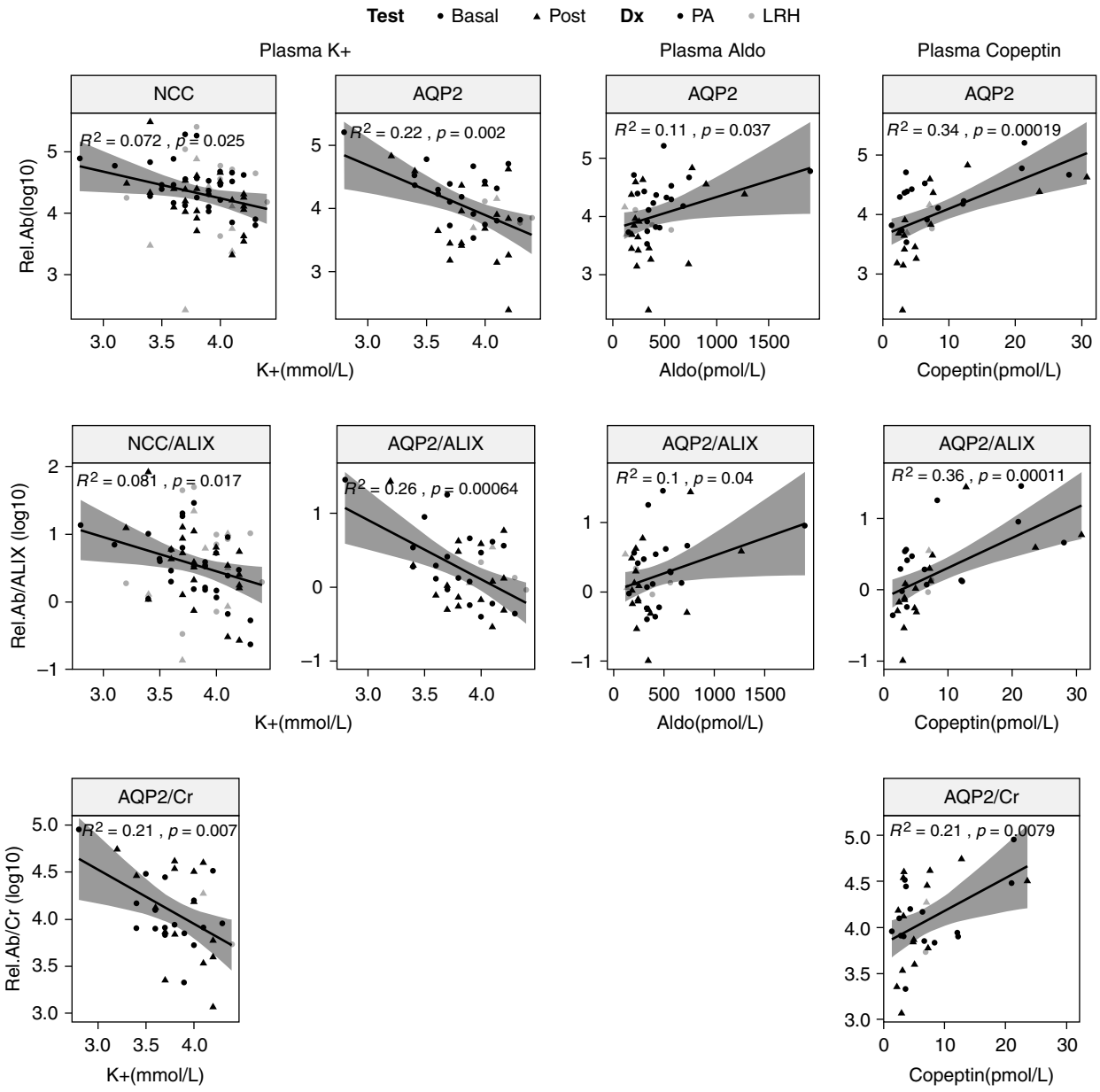

Figure 5. | **Notable correlations between plasma variables and immunoblotting-analyzed proteins of interest in all participants.** The first two columns demonstrate negative correlations between plasma potassium (K^+) and NCC, ALIX-corrected NCC (NCC/ALIX), AQP2, ALIX-corrected AQP2 (AQP2/ALIX), and creatinine-corrected AQP2 (AQP2/Cr). The third column shows positive correlations between plasma aldosterone (Aldo) and AQP2 and ALIX-corrected AQP2 (AQP2/ALIX). The last column shows positive correlations between plasma copeptin and AQP2, ALIX-corrected AQP2 (AQP/ALIX), and creatinine-corrected AQP2 (AQP/Cr). Dx, SSST diagnosis; Rel.Ab, protein relative abundance; Rel.Ab/ALIX, protein relative abundance corrected for ALIX; Rel.Ab/Cr, protein relative abundance corrected for spot urine creatinine concentration.

Disclosures

R.A. Fenton reports serving as an associate editor for the *American Journal of Physiology - Renal Physiology* and is an editorial board member of JASN. P.A. Welling reports having an advisory or leadership role on the renal editorial board of the *American Journal of Physiology*; receiving honoraria from the American Physiological Society; serving as chair of the finance committee of the American Physiological Society, and as chair of kidney molecular biology and development of the National Institutes of Health (NIH); and receiving research funding from the NIH. All remaining authors have nothing to disclose.

Funding

This work received funding from the Fondation Leducq Potassium in Hypertension grant.

Acknowledgment

We thank Mr. Andrew Jackson (Pathology Queensland) for performing tests of plasma Cl^- and HCO_3^-, and advice in data interpretation. A.Wu was supported by an Australian Government Research Training Program (RTP) Scholarship. R.A. Fenton was supported by the Novo Nordisk Fonden and the Danish Independent Research Fund: Medical Sciences.

Author Contributions

D. Cowley, R.A. Fenton, J. Palmfeldt, A. Wu, and Q. Wu were responsible for methodology; D. Cowley, J. Palmfeldt, A. Wu, and Q. Wu were responsible for data curation; R.A. Fenton, J. Palmfeldt, A. Wu, and Q. Wu were responsible for software; R.A. Fenton, M. Stowasser, P.A. Welling, M.J. Wolley, and A. Wu were responsible for funding acquisition and validation; R.A. Fenton, M. Stowasser, P.A. Welling, M.J. Wolley, and Q. Wu reviewed and edited the manuscript; R.A. Fenton, M. Stowasser, and M.J. Wolley provided supervision; R.A. Fenton, M. Stowasser, M.J. Wolley, A. Wu, and Q. Wu were responsible for investigation; J. Palmfeldt, A. Wu, and Q. Wu were responsible for resources; M. Stowasser, M.J. Wolley, and A. Wu conceptualized the study; A. Wu wrote the original draft and was responsible for project administration and visualization; and A. Wu and Q. Wu were responsible for formal analysis.

Data Sharing Statement

The LC-MS/MS proteomics data (Supplemental Appendix 2) have been deposited to the ProteomeXchange Consortium *via* the PRIDE partner repository with the dataset identifier PXD022653 (43).

Supplemental Material

This article contains supplemental material online at http://kidney360.asnjournals.org/lookup/suppl/doi:10.34067/KID.0000362022/-/DCSupplemental.

Supplemental Appendix 1. Detailed methods in the current study.

Supplemental Appendix 2. The LC-MS/MS proteomics data.

Supplemental Figure 1. Flow diagram of report numbers of individuals at each stage of study.

Supplemental Figure 2. A heatmap clustering of 294 differentially expressed proteins during SSST in PA and LRH subjects.

Supplemental Figure 3. Functional enrichment analyses of the 878 DEPs.

Supplemental Figure 4. Correlations between biochemical parameters and the 12 differentially expressed renal transmembrane proteins.

Supplemental Figure 5. Immunoblots of analysed proteins.

Supplemental Figure 6. Correlations between biochemical parameters and NCC, pNCC and AQP2.

Supplemental Figure 7. Boxplots of changes in the total contents in the urine during SSST.

Supplemental Figure 8. Correlations between EV markers (quantified by immunoblotting and MS) and spot urine creatinine.

Supplemental Table 1. Participants' clinical features and antihypertensive drugs at baseline.

Supplemental Table 2. NTA measures of particle size and concentration of nine uEV samples.

Supplemental Table 3. Abbreviation list.

References

1. Matsubara M: Renal sodium handling for body fluid maintenance and blood pressure regulation. *Yakugaku Zasshi* 124: 301–309, 2004 https://doi.org/10.1248/yakushi.124.301
2. Hoorn EJ, Gritter M, Cuevas CA, Fenton RA: Regulation of the renal NaCl cotransporter and its role in potassium homeostasis. *Physiol Rev* 100: 321–356, 2020 https://doi.org/10.1152/physrev.00044.2018
3. Terker AS, Yarbrough B, Ferdaus MZ, Lazelle RA, Erspamer KJ, Meermeier NP, Park HJ, McCormick JA, Yang CL, Ellison DH: Direct and indirect mineralocorticoid effects determine distal salt transport. *J Am Soc Nephrol* 27: 2436–2445, 2016 https://doi.org/10.1681/ASN.2015070815
4. Xu N, Hirohama D, Ishizawa K, Chang WX, Shimosawa T, Fujita T, Uchida S, Shibata S: Hypokalemia and pendrin induction by aldosterone. *Hypertension* 69: 855–862, 2017 https://doi.org/10.1161/HYPERTENSIONAHA.116.08519
5. Wolley MJ, Wu A, Xu S, Gordon RD, Fenton RA, Stowasser M: In primary aldosteronism, mineralocorticoids influence exosomal sodium-chloride cotransporter abundance. *J Am Soc Nephrol* 28: 56–63, 2017 https://doi.org/10.1681/ASN.2015111221
6. Wu A, Wolley MJ, Wu Q, Gordon RD, Fenton RA, Stowasser M: The Cl^-/HCO_3^- exchanger pendrin is downregulated during oral co-administration of exogenous mineralocorticoid and KCl in patients with primary aldosteronism. *J Hum Hypertens* 35: 837–848, 2021 https://doi.org/10.1038/s41371-020-00439-7
7. Qi Y, Wang X, Rose KL, MacDonald WH, Zhang B, Schey KL, Luther JM: Activation of the endogenous renin-angiotensin-aldosterone system or aldosterone administration increases urinary exosomal sodium channel excretion. *J Am Soc Nephrol* 27: 646–656, 2016 https://doi.org/10.1681/ASN.2014111137
8. Rozansky DJ, Cornwall T, Subramanya AR, Rogers S, Yang YF, David LL, Zhu X, Yang CL, Ellison DH: Aldosterone mediates activation of the thiazide-sensitive Na-Cl cotransporter through an SGK1 and WNK4 signaling pathway. *J Clin Invest* 119: 2601–2612, 2009 https://doi.org/10.1172/JCI38323
9. Stowasser M, Ahmed AH, Cowley D, Wolley M, Guo Z, McWhinney BC, Ungerer JP, Gordon RD: Comparison of seated with recumbent saline suppression testing for the diagnosis of primary aldosteronism. *J Clin Endocrinol Metab* 103: 4113–4124, 2018 https://doi.org/10.1210/jc.2018-01394
10. Ahmed AH, Cowley D, Wolley M, Gordon RD, Xu S, Taylor PJ, Stowasser M: Seated saline suppression testing for the diagnosis of primary aldosteronism: A preliminary study. *J Clin Endocrinol Metab* 99: 2745–2753, 2014 https://doi.org/10.1210/jc.2014-1153
11. van der Lubbe N, Jansen PM, Salih M, Fenton RA, van den Meiracker AH, Danser AH, Zietse R, Hoorn EJ: The phosphorylated sodium chloride cotransporter in urinary exosomes is superior to prostasin as a marker for aldosteronism. *Hypertension* 60: 741–748, 2012 https://doi.org/10.1161/HYPERTENSIONAHA.112.198135
12. Wu Q, Poulsen SB, Murali SK, Grimm PR, Su XT, Delpire E, Welling PA, Ellison DH, Fenton RA: Large-scale proteomic assessment of urinary extracellular vesicles highlights their reliability in reflecting protein changes in the kidney. *J Am Soc Nephrol* 32: 2195–2209, 2021 https://doi.org/10.1681/ASN.2020071035
13. Huebner A, Somparn P, Benjachat T, Leelahavanichkul A, Avihingsanon Y, Fenton R, Pisitkun T: Exosomes in Urine Biomarker Discovery. In: *Urine Proteomics in Kidney Disease Biomarker Discovery*, edited by Gao Y, Dordrecht, The Netherlands, Springer, 2015, pp 43–58 https://doi.org/10.1007/978-94-017-9523-4_5
14. Spanu S, van Roeyen CR, Denecke B, Floege J, Mühlfeld AS: Urinary exosomes: A novel means to non-invasively assess changes in renal gene and protein expression. *PLoS One* 9: e109631, 2014 https://doi.org/10.1371/journal.pone.0109631
15. Barros ER, Carvajal CA: Urinary exosomes and their cargo: Potential biomarkers for mineralocorticoid arterial hypertension? *Front Endocrinol (Lausanne)* 8: 230, 2017 https://doi.org/10.3389/fendo.2017.00230
16. Thuzar M, Young K, Ahmed AH, Ward G, Wolley M, Guo Z, Gordon RD, McWhinney BC, Ungerer JP, Stowasser M: Diagnosis of primary aldosteronism by seated saline suppression test-variability between immunoassay and HPLC-MS/MS. *J Clin Endocrinol Metab* 105: e477–e483, 2020 https://doi.org/10.1210/clinem/dgz150
17. Guo Z, Poglitsch M, McWhinney BC, Ungerer JPJ, Ahmed AH, Gordon RD, Wolley M, Stowasser M: Measurement of equilibrium angiotensin II in the diagnosis of primary aldosteronism. *Clin Chem* 66: 483–492, 2020 https://doi.org/10.1093/clinchem/hvaa001
18. Wiśniewski JR, Zougman A, Nagaraj N, Mann M: Universal sample preparation method for proteome analysis. *Nat Methods* 6: 359–362, 2009 https://doi.org/10.1038/nmeth.1322

19. Lee JW, Chou CL, Knepper MA: Deep sequencing in microdissected renal tubules identifies nephron segment-specific transcriptomes. *J Am Soc Nephrol* 26: 2669–2677, 2015 https://doi.org/10.1681/ASN.2014111067
20. Odorizzi G: The multiple personalities of Alix. *J Cell Sci* 119: 3025–3032, 2006 https://doi.org/10.1242/jcs.03072
21. Blijdorp CJ, Tutakhel OAZ, Hartjes TA, van den Bosch TPP, van Heugten MH, Rigalli JP, Willemsen R, Musterd-Bhaggoe UM, Barros ER, Carles-Fontana R, Carvajal CA, Arntz OJ, van de Loo FAJ, Jenster G, Clahsen-van Groningen MC, Cuevas CA, Severs D, Fenton RA, van Royen ME, Hoenderop JGJ, Bindels RJM, Hoorn EJ: Comparing approaches to normalize, quantify, and characterize urinary extracellular vesicles. *J Am Soc Nephrol* 32: 1210–1226, 2021 https://doi.org/10.1681/ASN.2020081142
22. Pizzolo F, Chiecchi L, Morandini F, Castagna A, Zorzi F, Zaltron C, Pattini P, Chiariello C, Salvagno G, Olivieri O: Increased urinary excretion of the epithelial Na channel activator prostasin in patients with primary aldosteronism. *J Hypertens* 35: 355–361, 2017 https://doi.org/10.1097/HJH.0000000000001168
23. Bruns JB, Carattino MD, Sheng S, Maarouf AB, Weisz OA, Pilewski JM, Hughey RP, Kleyman TR: Epithelial Na+ channels are fully activated by furin- and prostasin-dependent release of an inhibitory peptide from the gamma-subunit. *J Biol Chem* 282: 6153–6160, 2007 https://doi.org/10.1074/jbc.M610636200
24. Huebner AR, Cheng L, Somparn P, Knepper MA, Fenton RA, Pisitkun T: Deubiquitylation of protein cargo is not an essential step in exosome formation. *Mol Cell Proteomics* 15: 1556–1571, 2016 https://doi.org/10.1074/mcp.M115.054965
25. Stowasser M, Gordon RD: Primary aldosteronism: Changing definitions and new concepts of physiology and pathophysiology both inside and outside the kidney. *Physiol Rev* 96: 1327–1384, 2016 https://doi.org/10.1152/physrev.00026.2015
26. Dhondt B, Geeurickx E, Tulkens J, Van Deun J, Vergauwen G, Lippens L, Miinalainen I, Rappu P, Heino J, Ost P, Lumen N, De Wever O, Hendrix A: Unravelling the proteomic landscape of extracellular vesicles in prostate cancer by density-based fractionation of urine. *J Extracell Vesicles* 9: 1736935, 2020 https://doi.org/10.1080/20013078.2020.1736935
27. Arroyo JP, Lagnaz D, Ronzaud C, Vázquez N, Ko BS, Moddes L, Ruffieux-Daidié D, Hausel P, Koesters R, Yang B, Stokes JB, Hoover RS, Gamba G, Staub O: Nedd4-2 modulates renal Na^+-Cl^- cotransporter via the aldosterone-SGK1-Nedd4-2 pathway. *J Am Soc Nephrol* 22: 1707–1719, 2011 https://doi.org/10.1681/ASN.2011020132
28. Ronzaud C, Loffing-Cueni D, Hausel P, Debonneville A, Malsure SR, Fowler-Jaeger N, Boase NA, Perrier R, Maillard M, Yang B, Stokes JB, Koesters R, Kumar S, Hummler E, Loffing J, Staub O: Renal tubular NEDD4-2 deficiency causes NCC-mediated salt-dependent hypertension. *J Clin Invest* 123: 657–665, 2013 https://doi.org/10.1172/JCI61110
29. Lagnaz D, Arroyo JP, Chávez-Canales M, Vázquez N, Rizzo F, Spirlí A, Debonneville A, Staub O, Gamba G: WNK3 abrogates the NEDD4-2-mediated inhibition of the renal Na^+-Cl^- cotransporter. *Am J Physiol Renal Physiol* 307: F275–F286, 2014 https://doi.org/10.1152/ajprenal.00574.2013
30. McCormick JA, Bhalla V, Pao AC, Pearce D: SGK1: A rapid aldosterone-induced regulator of renal sodium reabsorption. *Physiology (Bethesda)* 20: 134–139, 2005 https://doi.org/10.1152/physiol.00053.2004
31. Terker AS, Ellison DH: Renal mineralocorticoid receptor and electrolyte homeostasis. *Am J Physiol Regul Integr Comp Physiol* 309: R1068–R1070, 2015 https://doi.org/10.1152/ajpregu.00135.2015
32. Czogalla J, Vohra T, Penton D, Kirschmann M, Craigie E, Loffing J: The mineralocorticoid receptor (MR) regulates ENaC but not NCC in mice with random MR deletion. *Pflugers Arch* 468: 849–858, 2016 https://doi.org/10.1007/s00424-016-1798-5
33. Terker AS, Zhang C, Erspamer KJ, Gamba G, Yang CL, Ellison DH: Unique chloride-sensing properties of WNK4 permit the distal nephron to modulate potassium homeostasis. *Kidney Int* 89: 127–134, 2016 https://doi.org/10.1038/ki.2015.289
34. van der Lubbe N, Moes AD, Rosenbaek LL, Schoep S, Meima ME, Danser AH, Fenton RA, Zietse R, Hoorn EJ: K^+-induced natriuresis is preserved during Na^+ depletion and accompanied by inhibition of the Na^+-Cl^- cotransporter. *Am J Physiol Renal Physiol* 305: F1177–F1188, 2013 https://doi.org/10.1152/ajprenal.00201.2013
35. Higashijima Y, Sonoda H, Takahashi S, Kondo H, Shigemura K, Ikeda M: Excretion of urinary exosomal AQP2 in rats is regulated by vasopressin and urinary pH. *Am J Physiol Renal Physiol* 305: F1412–F1421, 2013 https://doi.org/10.1152/ajprenal.00249.2013
36. van der Lubbe N, Lim CH, Meima ME, van Veghel R, Rosenbaek LL, Mutig K, Danser AH, Fenton RA, Zietse R, Hoorn EJ: Aldosterone does not require angiotensin II to activate NCC through a WNK4-SPAK-dependent pathway. *Pflugers Arch* 463: 853–863, 2012 https://doi.org/10.1007/s00424-012-1104-0
37. Relman AS, Schwartz WB: The nephropathy of potassium depletion; a clinical and pathological entity. *N Engl J Med* 255: 195–203, 1956 https://doi.org/10.1056/NEJM195608022550501
38. Marples D, Frøkiaer J, Dørup J, Knepper MA, Nielsen S: Hypokalemia-induced downregulation of aquaporin-2 water channel expression in rat kidney medulla and cortex. *J Clin Invest* 97: 1960–1968, 1996 https://doi.org/10.1172/JCI118628
39. Khositseth S, Uawithya P, Somparn P, Charngkaew K, Thippamom N, Hoffert JD, Saeed F, Michael Payne D, Chen SH, Fenton RA, Pisitkun T: Autophagic degradation of aquaporin-2 is an early event in hypokalemia-induced nephrogenic diabetes insipidus. *Sci Rep* 5: 18311, 2015 https://doi.org/10.1038/srep18311
40. Kanno K, Sasaki S, Hirata Y, Ishikawa S, Fushimi K, Nakanishi S, Bichet DG, Marumo F: Urinary excretion of aquaporin-2 in patients with diabetes insipidus. *N Engl J Med* 332: 1540–1545, 1995 https://doi.org/10.1056/NEJM199506083322303
41. Pisitkun T, Shen RF, Knepper MA: Identification and proteomic profiling of exosomes in human urine. *Proc Natl Acad Sci U S A* 101: 13368–13373, 2004 https://doi.org/10.1073/pnas.0403453101
42. Lee MH, Moxey JE, Derbyshire MM, Ward GM, MacIsaac RJ, Sachithanandan N: Decrease in serum potassium levels post saline suppression test in primary aldosteronism: An under-recognised phenomenon? *J Hum Hypertens* 30: 664–665, 2016 https://doi.org/10.1038/jhh.2016.7
43. Perez-Riverol Y, Csordas A, Bai J, Bernal-Llinares M, Hewapathirana S, Kundu DJ, Inuganti A, Griss J, Mayer G, Eisenacher M, Pérez E, Uszkoreit J, Pfeuffer J, Sachsenberg T, Yilmaz S, Tiwary S, Cox J, Audain E, Walzer M, Jarnuczak AF, Ternent T, Brazma A, Vizcaíno JA: The PRIDE database and related tools and resources in 2019: Improving support for quantification data. *Nucleic Acids Res* 47: D442–D450, 2019 https://doi.org/10.1093/nar/gky1106

Received: January 18, 2022 **Accepted:** February 28, 2022

See related editorial, "uEVs: A Potential Tool for Examining Renal Epithelial Cells," on pages 796–798.